Magnetic Resonance Imaging 62 (2019) 152–158

Contents lists available at ScienceDirect

Magnetic Resonance Imaging

journal homepage: www.elsevier.com/locate/mri

Original contribution

Reproducibility of simultaneous imaging of intracranial and extracranial arterial vessel walls using an improved T1-weighted DANTE-SPACE sequence on a 3 T MR system

Liwen Wan[a,b,1], Na Zhang[a,1], Lei Zhang[a], Xiaojin Long[a], Seng Jia[a], Ye Li[a], Dong Liang[a], Hairong Zheng[a], Xin Liu[a,*]

[a] Paul C. Lauterbur Research Center for Biomedical Imaging, Shenzhen Institutes of Advanced Technology, Chinese Academy of Sciences, Shenzhen, People's Republic of China

[b] University of Chinese Academy of Sciences, Beijing, People's Republic of China

ARTICLE INFO

Keywords:
Intra- and extracranial simultaneous imaging
MR vessel wall imaging
DANTE-SPACE
Reproducibility
Morphologic measurement

ABSTRACT

Purpose: To systematically investigate the scan-rescan, intra-observer, and inter-observer reproducibility of an improved DANTE-SPACE sequence for the simultaneous assessment of intra- and extracranial arterial vessel wall morphology.

Materials and methods: Thirty-five healthy volunteers and 10 patients with atherosclerotic plaque formation were each scanned twice using a T1-weighted DANTE-SPACE sequence on a 3 T MR system equipped with a 32-channel combined head and neck coil. Reproducibility analyses were performed for measurements of lumen and vessel wall volume, mean and maximum wall thickness, as well as for the normalized wall index. Intracranial and extracranial arterial segments were compared.

Results: Intra-class correlation coefficients (ICC) and Bland-Altman plots indicated good to excellent reproducibility for all morphologic measurements (all ICCs > 0.77). In addition, the range of ICCs of extracranial arteries (0.80–0.99) was significant higher than that of intracranial arteries (0.77–0.98, $P = 0.003$). The range of ICCs of patients (0.79–0.99) was generally higher than that of volunteers (0.77–0.99, $P = 0.47$), especially for extracranial arteries.

Conclusions: The improved T1-weighted DANTE-SPACE sequence is a reproducible method for the simultaneous assessment of intra- and extracranial vessel wall using a single MR scan. This method could potentially be used for assessing responses to therapy and for monitoring disease progression.

1. Introduction

Stroke is a common cause of death worldwide, and 80% of strokes are ischemic stroke [1]. Thrombosis caused by atherosclerotic plaque rupture is the main cause of ischemic stroke. Findings from a study in China indicate that 46.6% of culprit plaques originate from intracranial arteries, and 27.9% are derived from carotid arteries [2,3]. As one of the most promising noninvasive modalities for intracranial and carotid vessel wall imaging, MR scanning has been widely recognized by experts and is recommended by the American Society of Neuroradiology for current clinical practice [4,5].

In recent years, several high-resolution 3D isotropic black-blood sequences such as 3D variable-flip-angle TSE (SPACE) and 3D Motion Sensitized Driven Equilibrium (MSDE) prepared Rapid Gradient Echo (3D-MERGE), have been introduced to image either intracranial [6–11] or extracranial carotid [12,13] vessel walls. More recently, MR vessel wall scanning using large spatial coverage to simultaneously image intracranial and extracranial arterial vessel walls has been proposed [14]. By combining SPACE readout with Delay Alternating with Nutation for Tailored Excitation (DANTE-SPACE), the common carotid artery and the distal intracranial artery can be visualized in a single 3D scan. However, evaluation of cerebrospinal fluid (CSF) suppression using this method has been limited to the cervical spinal cord region. In addition, the low spatial resolution typically used has made depiction of distal middle cerebral arteries (MCA) difficult. To uniformly suppress CSF around the MCA, as well as blood flow at the carotid region, an

* Corresponding author at: Shenzhen Institutes of Advanced Technology, Chinese Academy of Sciences, 1068 Xueyuan Ave., Shenzhen University Town, Shenzhen 518055, People's Republic of China.

E-mail address: xin.liu@siat.ac.cn (X. Liu).

[1] These authors contributed equally to this work and should be considered co-first authors.

https://doi.org/10.1016/j.mri.2019.04.016
Received 29 January 2019; Received in revised form 29 March 2019; Accepted 29 April 2019

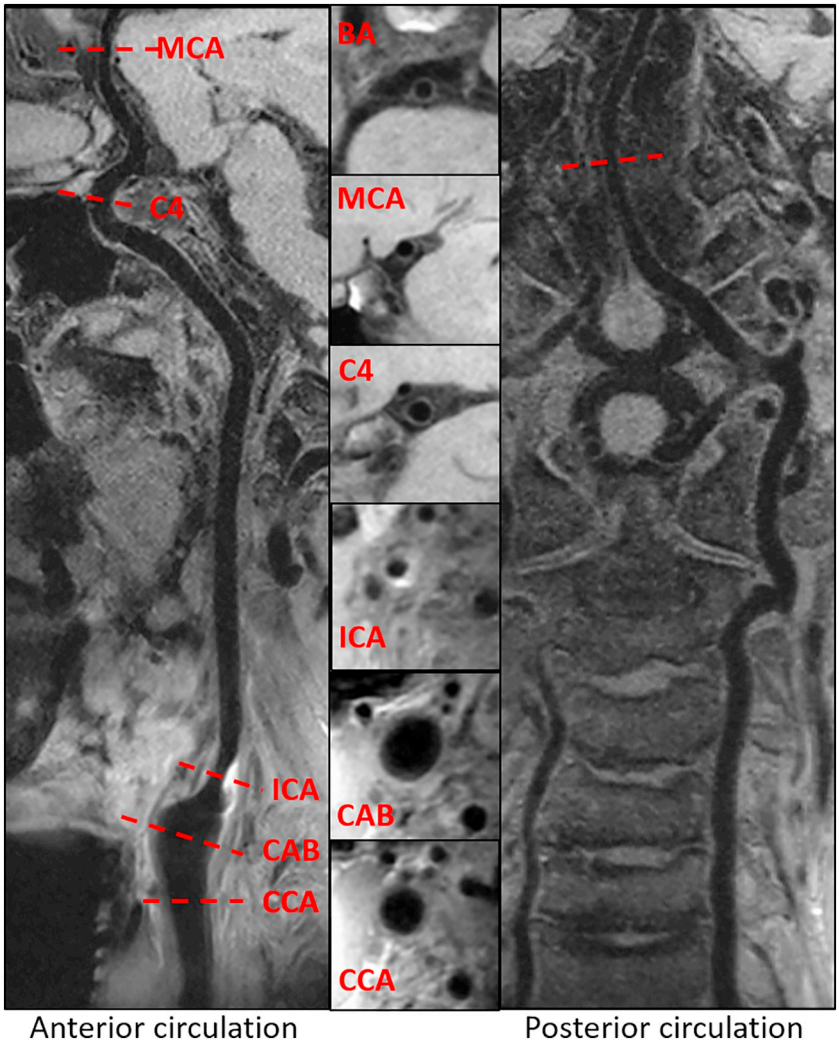

Fig. 1. Representative images acquired by the DANTE-SPACE sequence from a 68-year-old male patient. Six reconstructed image planes used for quantitative measurement are shown. A plaque in the ICA segment was detected with high T1 signal intensity. CCA = common carotid artery; CAB = carotid artery bifurcation; ICA = internal carotid artery; BA = distal basilar artery; C4 = distal intracranial carotid artery supraclinoid segment; MCA = middle cerebral artery.

improved DANTE-SPACE method was developed that achieved an isotropic spatial resolution of 0.55 mm [15]. The purpose of this current study was to evaluate the scan-rescan, and intra- and inter-observer reproducibility using this improved DANTE-SPACE method for the comprehensive assessment of intra- and extracranial arterial vessel wall morphology.

2. Material and methods

2.1. Study subjects

This study was IRB approved by Shenzhen Institutes of Advanced Technology and informed consent was obtained from each subject. In total, 35 volunteers (19 males, mean age 37 years, range 21–69 years) without any vascular disease and 10 patients (7 males, mean age 44 years, range 27–68 years) with clinically confirmed atherosclerotic disease were recruited for the study.

2.2. Imaging protocol

Each subject was scanned twice using the improved DANTE-SPACE prototype sequence on a 3 T MR system (TRIO, Siemens, Germany) equipped with a 32-channel head (24 channels) and neck (4 channels on each side) coil (Suzhou Medcoil Healthcare, China). The flip-down pulse was reinstated at the end of echo train to suppress CSF uniformly and improve T1 contrast [15,16], while the flip angles for the refocusing pulse series were calculated using T1/T2 = 1000 ms/150 ms; different T1/T2, 940 ms/100 ms, had been used in an earlier study [7]. The new refocusing pulse series increased signal intensity at the prescribed TE which made up for the signal loss from use of the flip-down pulse. The scan parameters were as follows: TE/TR = 23/1140 ms; spatial resolution = 0.55 × 0.55 × 0.55 mm^3; FOV = 180 × 212 mm^2; number of slices = 256; parallel imaging accelerate factor = GRAPPA 2, turbo factor = 48, echo spacing = 4.32 ms; bandwidth = 595 Hz/pixel; scan time = 9 min 6 s. The parameters for the DANTE preparation include: flip angle = 8°, phase increment = 0°, number of pulses = 150, interpulse repeat time = 1.5 ms, Gxyz = 20 mT/m. The time interval between the two scans for each subject was 1–2 weeks (mean 1.4 weeks) for volunteers and 1–20 weeks (mean 10 weeks) for patients.

2.3. Data analysis

Three carotid arterial segments and three intracranial arterial segments of each subject were used for morphological measurements. Fig. 1 presents a schematic of these six image segments used in the quantitative measurements. Specifically, the following three extracranial segments were identified: the common carotid artery (CCA,

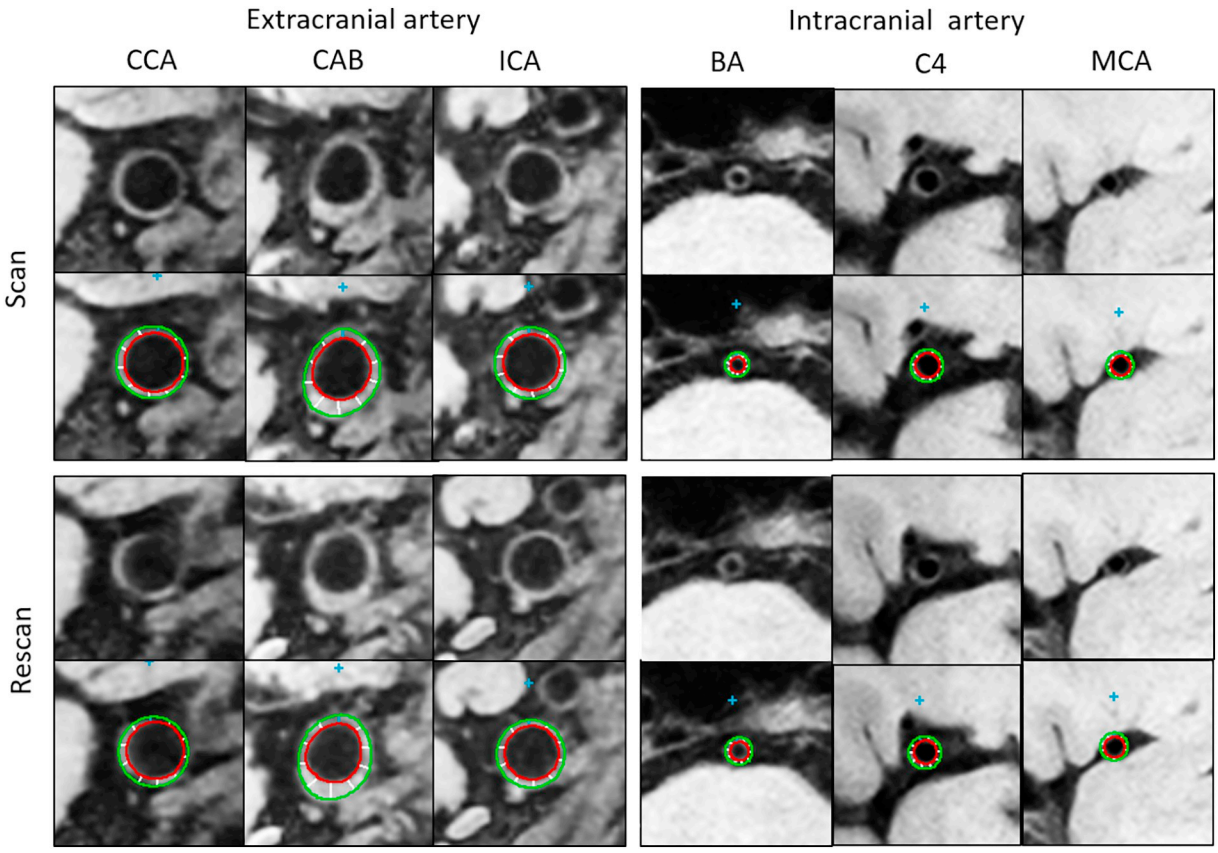

Fig. 2. Representative analytical images of scans and rescans of lumen and outer wall boundaries for the six designated arterial segments from a 48-year-old female patient. CCA = common carotid artery; CAB = carotid artery bifurcation; ICA = internal carotid artery; BA = distal basilar artery; C4 = distal intracranial carotid artery supraclinoid segment; MCA = middle cerebral artery.

Table 1
Inter-scan, intra-observer, and inter-observer reproducibility for intracranial and extracranial morphological measurements in healthy volunteers.

	Inter-scan (n = 102)			Intra-observer (*n* = 102)		Inter-observer (n = 102)	
	1st scan, 1st observer, 1st measurement (mean ± SD)	2nd scan, 1st observer (mean ± SD)	ICC (95% CI)	1st scan, 1st observer, 2nd measurement (mean ± SD)	ICC (95% CI)	1st scan, 2nd observer (mean ± SD)	ICC (95% CI)
Intracranial arteries (BA, C4, MCA)							
Mean wall thickness (mm)	0.52 ± 0.08	0.51 ± 0.08	0.86 (0.75–0.94)	0.52 ± 0.09	0.90 (0.79–0.95)	0.53 ± 0.09	0.80 (0.71–0.89)
Maximum wall thickness (mm)	0.67 ± 0.08	0.65 ± 0.08	0.83 (0.76–0.89)	0.66 ± 0.08	0.85 (0.78–0.90)	0.66 ± 0.09	0.77 (0.66–0.84)
Lumen volume (cm^3)	0.03 ± 0.01	0.03 ± 0.01	0.96 (0.94–0.97)	0.03 ± 0.01	0.98 (0.97–0.99)	0.03 ± 0.01	0.96 (0.94–0.97)
Wall volume (cm^3)	0.02 ± 0.007	0.02 ± 0.006	0.88 (0.82–0.92)	0.02 ± 0.006	0.93 (0.90–0.96)	0.02 ± 0.007	0.86 (0.79–0.90)
Normalized wall index	0.43 ± 0.05	0.42 ± 0.05	0.85 (0.78–0.90)	0.43 ± 0.06	0.86 (0.79–0.89)	0.43 ± 0.06	0.78 (0.69–0.89)
Extracranial arteries (CCA, CAB, ICA)							
Mean wall thickness (mm)	0.71 ± 0.14	0.69 ± 0.12	0.91 (0.86–0.94)	0.71 ± 0.14	0.94 (0.83–0.98)	0.73 ± 0.11	0.82 (0.76–0.89)
Maximum wall thickness (mm)	0.89 ± 0.15	0.86 ± 0.14	0.87 (0.81–0.91)	0.89 ± 0.16	0.88 (0.83–0.92)	0.87 ± 0.18	0.80 (0.73–0.87)
Lumen volume (cm^3)	0.12 ± 0.04	0.12 ± 0.04	0.99 (0.98–0.99)	0.12 ± 0.04	0.99 (0.99–0.99)	0.12 ± 0.04	0.97 (0.95–0.98)
Wall volume (cm^3)	0.05 ± 0.01	0.05 ± 0.01	0.93 (0.90–0.95)	0.05 ± 0.01	0.95 (0.93–0.97)	0.05 ± 0.01	0.83 (0.76–0.89)
Normalized wall index	0.30 ± 0.05	0.29 ± 0.04	0.87 (0.80–0.91)	0.30 ± 0.05	0.91 (0.86–0.94)	0.31 ± 0.05	0.84 (0.76–0.89)

SD = standard deviation; ICC = intra-class correlation coefficient; CI = confidence intervals; CCA = common carotid artery; CAB = carotid artery bifurcation; ICA = internal carotid artery; BA = distal basilar artery; C4 = distal intracranial carotid artery supraclinoid segment; MCA = middle cerebral artery.

Table 2
Inter-scan, intra-observer, and inter-observer reproducibility for intracranial and extracranial morphological measurements of patients.

	Inter-scan (n = 30)			Intra-observer (*n* = 30)		Inter-observer (n = 30)	
	1st scan, 1st observer, 1st measurement (mean ± SD)	2nd scan, 1st observer (mean ± SD)	ICC (95% CI)	1st scan, 1st observer, 2nd measurement (mean ± SD)	ICC (95% CI)	1st scan, 2nd observer (mean ± SD)	ICC (95% CI)
Intracranial arteries (BA, C4, MCA)							
Mean wall thickness (mm)	0.66 ± 0.09	0.67 ± 0.09	0.81 (0.61–0.91)	0.66 ± 0.08	0.83 (0.63–0.92)	0.66 ± 0.09	0.79 (0.63–0.90)
Maximum wall thickness (mm)	0.81 ± 0.11	0.80 ± 0.11	0.79 (0.67–0.90)	0.80 ± 0.09	0.83 (0.64–0.92)	0.81 ± 0.11	0.78 (0.66–0.90)
Lumen volume (cm^3)	0.03 ± 0.01	0.03 ± 0.01	0.96 (0.94–0.98)	0.03 ± 0.01	0.98 (0.97–0.99)	0.03 ± 0.01	0.98 (0.95–0.99)
Wall volume (cm^3)	0.03 ± 0.01	0.03 ± 0.01	0.90 (0.79–0.95)	0.03 ± 0.01	0.90 (0.79–0.95)	0.03 ± 0.01	0.83 (0.64–0.92)
Normalized wall index	0.50 ± 0.06	0.51 ± 0.06	0.86 (0.71–0.93)	0.50 ± 0.06	0.86 (0.71–0.93)	0.50 ± 0.06	0.83 (0.64–0.92)
Extracranial arteries (CCA, CAB, ICA)							
Mean wall thickness (mm)	1.00 ± 0.17	0.97 ± 0.16	0.92 (0.83–0.96)	0.99 ± 0.17	0.95 (0.93–0.96)	0.96 ± 0.12	0.87 (0.80–0.91)
Maximum wall thickness (mm)	1.36 ± 0.32	1.32 ± 0.32	0.86 (0.75–0.94)	1.35 ± 0.33	0.95 (0.91–0.98)	1.34 ± 0.29	0.95 (0.90–0.98)
Lumen volume (cm^3)	0.12 ± 0.06	0.12 ± 0.05	0.98 (0.96–0.99)	0.12 ± 0.05	0.99 (0.99–0.99)	0.13 ± 0.06	0.99 (0.98–0.99)
Wall volume (cm^3)	0.08 ± 0.02	0.07 ± 0.02	0.95 (0.90–0.98)	0.07 ± 0.02	0.96 (0.91–0.98)	0.07 ± 0.02	0.92 (0.83–0.96)
Normalized wall index	0.40 ± 0.07	0.39 ± 0.05	0.93 (0.90–0.95)	0.39 ± 0.06	0.96 (0.92–0.98)	0.38 ± 0.05	0.86 (0.71–0.94)

SD = standard deviation; ICC = intra-class correlation coefficient; CI = confidence intervals; CCA = common carotid artery; CAB = carotid artery bifurcation; ICA = internal carotid artery; BA = distal basilar artery; C4 = distal intracranial carotid artery supraclinoid segment; MCA = middle cerebral artery.

5 mm below the bifurcation), carotid artery bifurcation (CAB), and the internal carotid artery (ICA, 5 mm above the bifurcation). For each of these segments, five contiguous slices of 0.55 mm thickness same as imaging slice thickness were reformatted for the subsequent quantitative measurement. For intracranial vessels, the following three segments were identified: the distal basilar artery (BA); the distal intracranial carotid artery supraclinoid segment (C4); and the proximal middle cerebral artery (MCA). Two contiguous slices of 2 mm thickness were reformatted for each of these three segments delineating cross-sectional views of each vessel segment. Reformatting a thicker slice thickness for intracranial artery was to ensure a more accurate measurement due to the small size of the intracranial artery. All reformatted images were analyzed offline using a custom software VesselMASS (Leiden University Medical Center, Leiden, the Netherlands). The contours of the lumen and outer wall boundaries were semi-automatically generated and divided into ten segments, as shown in Fig. 2. Mean and maximum wall thickness were automatically calculated as the mean and maximum value of the distance between the lumen and outer contours measured from these ten evenly distributed segments. The lumen area was calculated as the area inside the luminal contour. The wall area was calculated by subtracting the lumen area from the outer contour area. Normalized wall index was defined as the ratio of vessel wall area to the total vessel area (the outer contour area). For each arterial segment, the normalized wall index and mean/maximum wall thickness were, respectively, averaged over the two or five slices; lumen volume and wall volume were obtained by summing the area measurements of the two or five slices and multiplying by 2 mm or 0.55 mm (slice thickness), respectively. To test the scan–rescan reproducibility, all images were analyzed by a highly trained observer with two years of vascular MRI experience. To test intra-observer reproducibility, the first scan was analyzed twice in a two-week time span by the same observer. The first scan was also analyzed by a second observer with six years of vascular MRI experience, to compare the inter-observer reproducibility to the first measurement of the first observer. In addition, the cohort was further categorized into two groups for comparison of reproducibility by segment (intracranial and extracranial arterial segments) and health status (patients and healthy volunteers), respectively.

2.4. Statistical analysis

Statistical analyses were performed using SPSS (v.19.0; SPSS, Chicago, IL, USA) statistical software. Intra-class correlation coefficients (ICCs) and 95% confident intervals (CIs) were calculated to evaluate the reproducibility of wall and lumen volume measurements, normalized wall index, and wall thickness between repeated scans and measurements. ICC values of < 0.5, between 0.5 and 0.75, between 0.75 and 0.9, and > 0.90 were indicative of poor, moderate, good, and excellent reliability, respectively [17]. Mann-Whitney *U* Test was used to examine the difference of ICCs between intracranial and extracranial arteries, as well as volunteers and patients. Statistical significance was defined at $P < 0.05$. Bland-Altman analysis was also used to determine the scan-rescan, intra-, and inter-observer reproducibility.

3. Results

All 45 subjects completed the MR examinations successfully. The simultaneous intra- and extracranial arterial vessel wall imaging method provided good delineation of both the intracranial and extracranial arterial wall (Fig. 1). Seven subjects performed repeat scans due to motion artifacts. But there was still blur on the images of one volunteer who was excluded from statistical analysis. A total of 264 paired arterial segments (132 image pairs for intracranial and 132 pairs for extracranial analysis) from 44 subjects were available for the quantitative analysis. There was no occlusive vascular segments existed in the patient group. Three patients had only carotid plaques and seven patients had only intracranial plaques. All the plaques were relatively small (type I –III according to modified AHA classification of atherosclerotic plaque [18]).

Table 1 summarizes the morphologic measurements and corresponding ICC values of intra- and extracranial segments for all volunteers. Each of the assessed morphologic indices had ICCs > 0.77, indicating good to excellent reproducibility. More specifically, for the intra-observer reproducibility, all ICCs were equal to or > 0.85. For scan-rescan reproducibility, all ICCs were equal to or > 0.83. The range of ICCs of extracranial arteries (0.80–0.99) was higher than that of

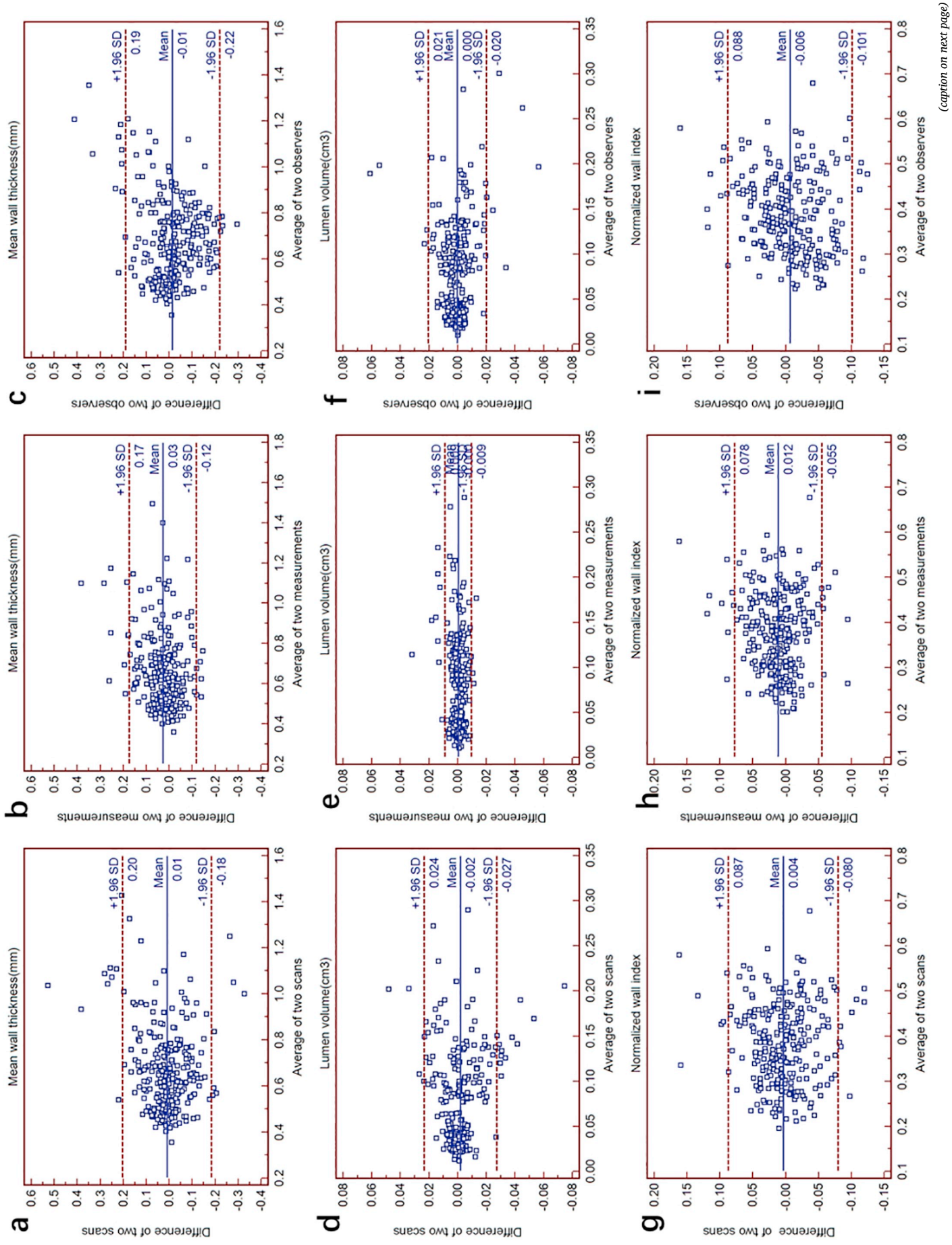

(caption on next page)

Fig. 3. Bland-Altman plots for mean wall thickness (a: inter-scan, b: intra-observer, c: inter-observer), lumen volume (d: inter-scan, e: intra-observer, f: inter-observer), and normalized wall index (g: inter-scan, h: intra-observer, i: inter-observer). The solid lines represent the mean difference, and the dashed lines indicate the 95% limits of agreement. Note good agreement was achieved for inter-scan, intra-observer and inter-observer measurements of mean wall thickness, lumen volume and normalized wall index. SD = standard deviation.

intracranial arteries (0.77–0.98), but there is no significant difference ($P = 0.048$).

Table 2 presents the morphologic measurements and corresponding ICC values of intra- and extracranial segments for patients. All ICCs were equal to or > 0.78, indicating good to excellent reproducibility. The corresponding range of ICC values of extracranial arteries (0.86–0.99) was significant higher than that of intracranial arteries (0.79–0.98) in all categories ($P = 0.004$). In addition, the ICCs of patients were generally higher than those of volunteers ($P = 0.47$), especially for the extracranial arteries.

For all analyses, inter-observer reproducibility was slightly lower but still good or excellent (all ICC values ≥077). Moreover, maximum wall thickness consistently had the smallest ICC values, and the lumen volume consistently had the largest ICC values. Segment-based results are summarized in Supplemental Table 1. The ICCs for each segment (0.80–0.99) were generally higher than those of the averages of overall assessed segments (0.77–0.99).

The Bland-Altman plots of mean wall thickness, lumen volume, and normalized wall index for all arterial segments are shown in Fig. 3. Random error scattering patterns and independence of the difference in the mean values were observed.

4. Discussion

In this study, both healthy volunteers and patients with atherosclerotic plaque formations were scanned with a DANTE-SPACE MR sequence for the simultaneous imaging of intra- and extracranial carotid vessel walls. The FOV of 180 × 212 mm^2 ensures one-stop scanning of all major arteries from the common carotid artery to M2 or M3 segment of MCA. The results indicate good to excellent reproducibility of scan-rescan, intra-observer, and inter-observer measurements of mean wall thickness, lumen volume, normalized wall index, and other morphological indices.

Non-invasive assessment of plaque progression and regression is clinically desirable for assessing treatment responses of patients having atherosclerotic complications. Plaque morphologic measurements derived from high-resolution vessel wall MR scans have proven to be as effective as the use of quantitative imaging markers for assessing intracranial and extracranial vascular beds [19–23]. All ICCs were equal or > 0.77 in this current study, results similar to previous studies where intracranial and carotid arteries were scanned using separate MR protocols [24–29]. Previous studies have shown that the lumen and wall area, lumen and wall volume, total vessel volume, mean and maximum wall thickness, and normalized wall index of the carotid artery assessed with better ICCs (≥0.87) [25]. The present study confirmed the reproducibility of the 3D T1-weighted sequence and our data showed slightly lower ICC values (≥0.80) for extracranial vessel wall assessment. This is likely because the 3D technique is more susceptible to any errors caused by, for example, image registration, reformation, and vessel wall contouring. For intracranial arteries, previous studies were focused on evaluating MCA lumen and plaque area and volume, which showed high reproducibility [27,28]. Our study included a large spatial coverage, and additional intracranial segments such as C4 and BA were also imaged and assessed.

The reproducibility of extracranial artery measurements (ICC range 0.80–0.99) was significantly higher than that of intracranial arteries (ICC range 0.77–0.98, $P = 0.003$). This is most likely attributable to thicker extracranial arteries (range 0.69–1.0 mm) relative to intracranial arteries (range 0.51–0.67 mm) and a reduced partial volume effect from this thicker vessel wall. The results also revealed higher reproducibility for patients (ICC range 0.79–0.99) compared to volunteers (ICC range 0.77–0.99). But there was no significant difference of the ICCs between patients and volunteers ($P = 0.47$). The reason may be that the plaques of the patients recruited to the study were relatively small, making the patient's wall thickness slightly thicker (range 0.66–1.0 mm) than the volunteer (range 0.51–0.73 mm). In addition, the ICCs for each segment were generally higher than for those averaged over all assessed segments. This is likely due to morphological differences in the three intracranial arterial segments (BA, C4, and MCA).

The reproducibility of the maximum wall thickness of all subjects was slightly lower (ICC = 0.80), which could be explained by the difficulty of measurement of wall thickness: spatial resolution, delineation of vessel wall boundaries, and segmentation of the vessel wall itself are all challenges to these measurements. In addition, the whole artery volume measurements were higher relative to other morphological measurements (all ICCs > 0.85). Thus, volume-based measurements would be preferable for clinical studies due to better reliability.

The following limitations need to be acknowledged. First, this study focused on healthy subjects; only ten patients were included. It would be ideal if more patients could be recruited to increase the statistical power of all measurements. Second, the inter-scan interval time for patient group was relatively long, which may cause some uncertainty. However, the plaques of the patients recruited to this study are relatively small and their progression are slow. This actually has little influence on the two repeated measurement results. Third, although scans and rescans were performed under stable conditions, only one type of MRI scanner and one type of software were used for vessel wall analysis. A multi-center reproducibility study is needed. Last, although the scan time is shorter than the time required for imaging intra- and extracranial vessel walls separately using conventional methods, the scan time of the technique is relatively long. In the future, faster imaging methods such as compression sensing will be considered to shorten the imaging time.

5. Conclusions

In conclusion, to our knowledge, this study provides the first comprehensive assessment of scan-rescan, intra-observer, and inter-observer reproducibility of simultaneous intracranial and extracranial vessel wall imaging using a single 3D measurement. The results indicate that the improved DANTE-SPACE technique is a reproducible MR method for simultaneous intra- and extracranial vessel wall imaging. Such a technique could potentially be used for assessing response to therapy and monitoring disease progression.

Supplementary data to this article can be found online at https://doi.org/10.1016/j.mri.2019.04.016.

Acknowledgement

This work was supported in part by National Natural Science Foundation of China (81830056, 81801691), Natural Science Foundation of Guangdong Province (2018A030313204), National Key R&D Program of China (2016YFC0100100), and Shenzhen Basic Research Program (JCYJ20170413161350892).

References

[1] Ga D, Fisher M, Macleod M, Davis SM. Stroke. Lancet 2008;371(9624):1612–23.
[2] Wang Y, Zhao X, Liu L, Soo YO, Pu Y, Pan Y, et al. Prevalence and outcomes of symptomatic intracranial large artery stenoses and occlusions in China: the Chinese Intracranial Atherosclerosis (CICAS) Study. Stroke 2014;45(3):663–9.
[3] Zhao X, Hippe DS, Li R, Canton GM, Sui B, Song Y, et al. Prevalence and characteristics of carotid artery high-risk atherosclerotic plaques in Chinese patients with cerebrovascular symptoms: a Chinese Atherosclerosis Risk Evaluation II Study. J Am Heart Assoc 2017;6(8):e005831.
[4] Mandell D, Mossa-Basha M, Qiao Y, Hess C, Hui F, Matouk C, et al. Intracranial vessel wall MRI: principles and expert consensus recommendations of the American Society of Neuroradiology. Am J Neuroradiol 2017;38(2):218–29.
[5] Saba L, Yuan C, Hatsukami T, Balu N, Qiao Y, DeMarco J, et al. Carotid artery wall imaging: perspective and guidelines from the ASNR vessel wall imaging study group and expert consensus recommendations of the American Society of Neuroradiology. Am J Neuroradiol 2018;39(2):E9–31.
[6] Qiao Y, Steinman DA, Qin Q, Etesami M, Schär M, Astor BC, et al. Intracranial arterial wall imaging using three-dimensional high isotropic resolution black blood MRI at 3.0 Tesla. J Magn Reson Imaging 2011;34(1):22–30.
[7] Zhang L, Zhang N, Wu J, Zhang L, Huang Y, Liu X, et al. High resolution three dimensional intracranial arterial wall imaging at 3 T using T1 weighted SPACE. Magn Reson Imaging 2015;33(9):1026–34.
[8] Zhao X, Li R, He L. Comprehensive vessel wall imaging for concomitant extracranial and intracranial atherosclerotic plaques in symptomatic patients using fast 3D multicontrast black-blood MR imaging sequences. ISMRM 21st annual meeting & exhibition, salt lake city, American. 2013.
[9] Fan Z, Yang Q, Deng Z, Li Y, Bi X, Song S, et al. Whole-brain intracranial vessel wall imaging at 3 Tesla using cerebrospinal fluid–attenuated T1-weighted 3 D turbo spin echo. Magn Reson Med 2017;77(3):1142–50.
[10] Li M-L, Xu Y-Y, Hou B, Sun Z-Y, Zhou H-L, Jin Z-Y, et al. High-resolution intracranial vessel wall imaging using 3D CUBE T1 weighted sequence. Eur J Radiol 2016;85(4):803–7.
[11] van der Kolk AG, Hendrikse J, Brundel M, Biessels GJ, Smit EJ, Visser F, et al. Multi-sequence whole-brain intracranial vessel wall imaging at 7.0 tesla. Eur Radiol 2013;23(11):2996–3004.
[12] Wang J, Börnert P, Zhao H, Hippe DS, Zhao X, Balu N, et al. Simultaneous non-contrast angiography and intraplaque hemorrhage (SNAP) imaging for carotid atherosclerotic disease evaluation. Magn Reson Med 2013;69(2):337–45.
[13] Fan Z, Zhang Z, Chung YC, Weale P, Zuehlsdorff S, Carr J, et al. Carotid arterial wall MRI at 3T using 3D variable-flip-angle turbo spin-echo (TSE) with flow-sensitive dephasing (FSD). J Magn Reson Imaging 2010;31(3):645–54.
[14] Xie Y, Yang Q, Xie G, Pang J, Fan Z, Li D. Improved black-blood imaging using DANTE-SPACE for simultaneous carotid and intracranial vessel wall evaluation. Magn Reson Med 2016;75(6):2286–94.
[15] Zhang L, Zhang N, Wu J, Liu X, Chung Y-C. High resolution simultaneous imaging of intracranial and extracranial arterial wall with improved cerebrospinal fluid suppression. Magn Reson Imaging 2017;44:65–71.
[16] Yang H, Zhang X, Qin Q, Liu L, Wasserman BA, Qiao Y. Improved cerebrospinal fluid suppression for intracranial vessel wall MRI. J Magn Reson Imaging 2016;44(3):665–72.
[17] Koo TK, Li MY. A guideline of selecting and reporting intraclass correlation coefficients for reliability research. J Chiropr Med 2016;15(2):155–63.
[18] Cai J-M, Hatsukami TS, Ferguson MS, Small R, Polissar NL, Yuan C. Classification of human carotid atherosclerotic lesions with in vivo multicontrast magnetic resonance imaging. Circulation 2002;106(11):1368–73.
[19] Qiao Y, Guallar E, Suri FK, Liu L, Zhang Y, Anwar Z, et al. MR imaging measures of intracranial atherosclerosis in a population-based study. Radiology 2016;280(3):860–8.
[20] Zhao X-Q, Dong L, Hatsukami T, Phan BA, Chu B, Moore A, et al. MR imaging of carotid plaque composition during lipid-lowering therapy: a prospective assessment of effect and time course. JACC Cardiovasc Imaging 2011;4(9):977–86.
[21] Underhill HR, Yuan C, Zhao X-Q, Kraiss LW, Parker DL, Saam T, et al. Effect of rosuvastatin therapy on carotid plaque morphology and composition in moderately hypercholesterolemic patients: a high-resolution magnetic resonance imaging trial. Am Heart J 2008;155(3):584. e1–584. [e8].
[22] Corti R, Worthley SG, Helft G, Viles-Gonzalez JF, Badimon JJ, Fuster V, et al. Effects of aggressive versus conventional lipid-lowering therapy by simvastatin on human atherosclerotic lesions: a prospective, randomized, double-blind trial with high-resolution magnetic resonance imaging. J Am Coll Cardiol 2005;46(1):106–12.
[23] Fernandes JL, Serrano Jr. CV, Blotta MHS, Coelho OR, Nicolau JC, Ávila LF, et al. Regression of coronary artery outward remodeling in patients with non-ST-segment acute coronary syndromes: a longitudinal study using noninvasive magnetic resonance imaging. Am Heart J 2006;152(6):1123–32.
[24] Alizadeh Dehnavi R, Doornbos J, Tamsma JT, Stuber M, Putter H, van der Geest RJ, et al. Assessment of the carotid artery by MRI at 3T: a study on reproducibility. Journal of Magnetic Resonance Imaging: An Official Journal of the International Society for Magnetic Resonance in Medicine 2007;25(5):1035–43.
[25] Li F, Yarnykh VL, Hatsukami TS, Chu B, Balu N, Wang J, et al. Scan-rescan reproducibility of carotid atherosclerotic plaque morphology and tissue composition measurements using multicontrast MRI at 3T. J Magn Reson Imaging 2010;31(1):168–76.
[26] Kröner E, Westenberg J, van der Geest R, Brouwer N, Doornbos J, Kooi M, et al. High field carotid vessel wall imaging: a study on reproducibility. Eur J Radiol 2013;82(4):680–5.
[27] Yang W-Q, Huang B, Liu X-T, Liu H-J, Li P-J, Zhu W-Z. Reproducibility of high-resolution MRI for the middle cerebral artery plaque at 3T. Eur J Radiol 2014;83(1):e49–55.
[28] Zhang X, Zhu C, Peng W, Tian B, Chen L, Teng Z, et al. Scan-rescan reproducibility of high resolution magnetic resonance imaging of atherosclerotic plaque in the middle cerebral artery. PLoS One 2015;10(8):e0134913.
[29] Zhang N, Zhang F, Deng Z, Yang Q, Diniz MA, Song SS, et al. 3D whole-brain vessel wall cardiovascular magnetic resonance imaging: a study on the reliability in the quantification of intracranial vessel dimensions. J Cardiovasc Magn Reson 2018;20(1):39.